

Enhancement of flux pinning and high-field critical current density in carbon-alloyed MgB₂ thin films

J. Chen,¹ V. Ferrando,^{1,2} P. Orgiani,^{1,3} A. V. Pogrebnyakov,^{1,4} R. H. T. Wilke,¹ J. B. Betts,⁵ C. H. Mielke,⁵ J. M. Redwing,⁴ X. X. Xi,^{1,4} and Qi Li^{1,*}

¹*Department of Physics, Pennsylvania State University, University Park, Pennsylvania 16802, USA*

²*University of Genoa/INFM-LAMIA, Genoa 16146, Italy*

³*CNR-INFM SuperMat, Baronissi (SA), I-84081, Italy*

⁴*Department of Materials Science and Engineering, Pennsylvania State University, University Park, Pennsylvania 16802, USA*

⁵*National High Magnetic Field Laboratory, Los Alamos National Laboratory, Los Alamos, New Mexico 87545, USA*

(Received 27 July 2006; published 16 November 2006)

We have studied flux pinning and critical current density in carbon-alloyed MgB₂ thin films prepared by hybrid physical-chemical vapor deposition. We found that carbon alloying significantly enhances flux pinning. The thermal activation energy of vortices $U(H)$ and critical current density $J_c(H)$ are much higher in carbon-alloyed films than in pure MgB₂ films at high fields. From the scaling behavior of the reduced pinning force with reduced field, we found that the dominant pinning mechanism changes from the grain boundary pinning in pure MgB₂ films to normal point pinning at low carbon content and back to grain boundary pinning at higher carbon contents for $H \perp ab$. No dominant pinning mechanism exists when $H \parallel ab$.

DOI: [10.1103/PhysRevB.74.174511](https://doi.org/10.1103/PhysRevB.74.174511)

PACS number(s): 74.70.Ad, 74.25.Qt, 74.25.Sv

I. INTRODUCTION

Magnesium diboride, with a superconductor transition temperature near 40 K,¹ has emerged to be a promising material for high-magnetic-field applications.² MgB₂ is a unique superconductor having two conduction bands and two superconducting gaps.³ Modifications of the interband and intraband scattering in MgB₂ can lead to significant enhancement of the upper critical field H_{c2} .⁴ Recently, we have shown in MgB₂ thin films prepared by hybrid physical-chemical vapor deposition (HPCVD)⁵ that alloying with carbon can dramatically enhance H_{c2} to 40 T in a perpendicular field and over 60 T in a parallel field (at 4.2 K).⁶ Such extraordinary H_{c2} values are not only higher than those in bulk Mg(B_{1-x}C_x)₂ (Ref. 7) and SiC-doped MgB₂,⁸ they are also well above those of standard high-field material Nb-based superconductors.² This raises the possibility of using MgB₂ to replace Nb-based compounds for superconducting magnets in, for example, magnetic resonance imaging (MRI) systems.

In order to be of practical use, a superconducting material must not only exhibit a high upper critical field, but also be able to carry large superconducting current densities ($>10^5$ A/cm²) in high magnetic fields.⁹ In the mixed state of a type II superconductor, magnetic flux penetrates the superconductor in the form of vortices. For the superconductor to carry dissipation-free current, the vortices have to be pinned by microstructural defects. At an irreversibility field H_{irr} , the Lorentz force on a vortex exceeds the pinning force $F_p = \mu_0 H J_c$, thus the vortices start to move, resulting in a voltage drop along the direction of the current flow, and hence the critical current vanishes. Increasing the upper critical field increases the difference in free energy between normal and superconducting regions and it follows that increasing H_{c2} should lead to an enhancement of the flux pinning. It should be noted that this holds only if the microstructure of the material, i.e., the nature and density of the pinning sites, is not significantly changed.

It is possible to infer the type of pinning from force pinning curves. If a dominant pinning mechanism exists, the field dependence of the pinning force is found to obey the general relationship $F_p \propto h^n(1-h)^m$, where n and m depend upon the particular type of pinning, and h is the reduced field, $h = H/H_{irr}$.^{10,11} Such scaling laws have been used to propose different pinning mechanisms, depending upon sample preparation, for MgB₂.¹²⁻¹⁴

While carbon substitution for boron has been shown to enhance the upper critical field in bulk MgB₂,^{15,16} reaction temperatures as high as 1200 °C are necessary to synthesize fully reacted, homogeneously doped, high density wire.⁷ The increase in reaction temperature resulted in a substantial coarsening of the grain size and, since in these samples grain boundary pinning is believed to be the dominant mechanism, an overall decrease in $J_c(H, T)$ compared to pure, undoped wires reacted at lower temperatures.⁷ Ensuring simultaneous enhancements of both H_{c2} and H_{irr} is therefore a nontrivial problem that needs to be addressed. In bulk MgB₂, H_{irr} enhancements have been reported for carbon-doped single crystals,¹⁷ and in polycrystalline wires synthesized either by hot isostatic pressing¹⁸ or by adding SiC nanoparticles.¹⁹ It is desirable to develop growth techniques to enhance both H_{c2} and H_{irr} in MgB₂ thin films, where H_{c2} values over 60 T, nearly double the value seen in bulk,^{7,16} have been reported.⁶ The recent discovery of high H_{c2} and H_{irr} values in randomly oriented polycrystalline carbon-alloyed MgB₂ wires grown by HPCVD²⁰ suggests the results obtained in thin films may also be achieved in bulk form. For randomly oriented bulk materials, $J_c(H)$ is highly dependent upon $H \perp ab$.²¹ It is therefore important to understand the pinning mechanisms in carbon-alloyed HPCVD films for the field direction $H \perp ab$, and to find out the ratio H_{irr}/H_{c2} for MgB₂, which is near 0.85 for Nb-based superconductors and much smaller for high-temperature superconductors.⁹ In this paper, we report a significant enhancement of H_{irr} for $H \perp ab$ by carbon alloying in HPCVD MgB₂ films. We found that the pinning

mechanism changes as the microstructure of the films evolves with increasing carbon content. The flux pinning is much stronger and the high-field critical current density much higher in carbon-alloyed films than in pure MgB₂ films. For $H \parallel ab$, we found no dominant pinning mechanism. However, the result of H_{irr} for $H \parallel ab$ from transport measurements is given for a carbon-alloyed MgB₂ film, which shows an H_{irr} for $H \parallel ab$ of 45 T at 4.2 K.

II. EXPERIMENTAL METHODS

The HPCVD MgB₂ films in this work were grown at 720 °C on (0001) 4H-SiC single-crystal substrates. The film thickness was around 2000 Å. The pure MgB₂ films are clean with low residual resistivity ρ_0 and high T_c (0.3–4 $\mu\Omega$ cm and \sim 41 K, respectively²²). For carbon alloying, we added bis(methylcyclopentadienyl)magnesium [(MeCp)₂Mg], a metalorganic magnesium precursor, to the gas flow in the HPCVD reactor.²³ Nominal carbon concentration was controlled by adjusting the rate of a secondary hydrogen flow passing through the (MeCp)₂Mg bubbler. Using wavelength dispersive x-ray spectroscopy (WDS) measurements, a correlation between the secondary hydrogen flow rate and the overall carbon content in the films was established (see Ref. 24). In this work, we present the results for pure MgB₂ films along with three carbon-doped films with overall atomic concentrations of 7.4%, 12%, and 15%. It should be noted that only a small fraction of the carbon enters the MgB₂ structure and a majority of the carbon precipitates out in the form of boron carbide (most likely B₄C, B₈C, or B₁₃C₂) or other amorphous phases in the grain boundaries.^{23,24} The result of H_{irr} for $H \parallel ab$ for one sample with 25% carbon concentration is also presented.

For transport measurements, the films were patterned into 30 $\mu\text{m} \times 60 \mu\text{m}$ bridges and the standard four-probe method was used. An ac current of 800 A/cm² and 17 Hz was used for the resistivity measurement. Carbon alloying increases resistivity and suppresses T_c . For the samples used in this work, ρ_0 and T_c were 4.2 $\mu\Omega$ cm and 41 K for the pure film, 19 $\mu\Omega$ cm and 39.8 K for the 7.4% carbon film, 47 $\mu\Omega$ cm and 38 K for the 12% carbon film, and 193 $\mu\Omega$ cm and 34 K for the 15% carbon film, respectively. Magnetic-field dependencies were measured on a Quantum Design PPMS system with a 9-T magnet. J_c was measured using a dc current with a voltage criterion of 1 μV . Measurement in pulsed magnetic field up to 60 T for the 25% carbon sample was carried out at the National High Magnetic Field Laboratory (NHMFL) at Los Alamos National Laboratory.

III. RESULTS AND DISCUSSION

The irreversibility fields in MgB₂ reported in the literature have been obtained in several different ways: by magnetization,²⁵ by resistivity criteria of 10% normal-state resistivity²⁶ or zero resistivity,²⁷ by J_c criteria of 10 A/cm² (Ref. 26) or 10³ A/cm²,²⁸ or by plotting $J^{1/2}H^{1/4}$ versus H .^{12,29} The intercept of a linear extrapolation of $J^{1/2}H^{1/4}$ versus H with the horizontal axis gives a good estimate of H_{irr} .^{12,29} Because the H_{irr} values of the carbon-alloyed

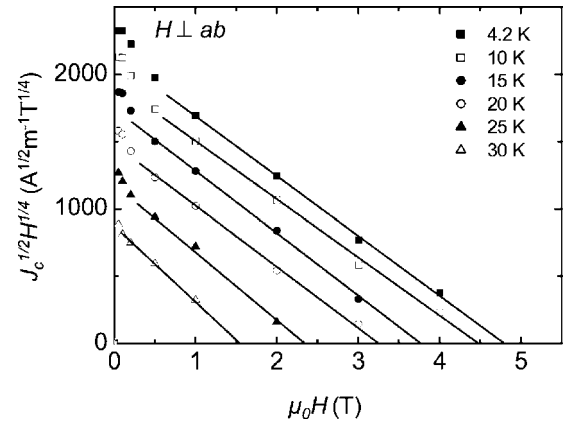


FIG. 1. $J_c^{1/2}H^{1/4}$ vs H , for pure MgB₂ films with the $H \perp ab$ plane. The solid lines are linear extrapolations to find the irreversibility fields.

HPCVD films at low temperatures are higher than the 9-T limit of our PPMS system, we used the $J^{1/2}H^{1/4}$ versus H plots to obtain H_{irr} .³⁰ For the pure MgB₂ film where the resistivity and J_c criteria can also be used, the H_{irr} values from the various methods are in agreement with each other. It should be noted that the linear dependence of $J^{1/2}H^{1/4}$ versus H applies to grain boundary pinning, limited by flux shear along the boundaries. As will be shown below, the force pinning curves for all but the nominal 7.4% carbon-doped sample support this assumption. The nominal 7.4% carbon-doped sample exhibits a force curve consistent with the dominant pinning mechanism being normal point pins. As a result, we used a modified formula, which is consistent with the shape of the flux pinning curve for this sample, namely $J_c^{1/2}$ versus H , to determine H_{irr} .

Figure 1 is a $J^{1/2}H^{1/4}$ versus H plot for a pure MgB₂ film with $H \perp ab$. $J^{1/2}H^{1/4}$ decreases linearly with H for large H (i.e., $H > 0.5$ T), from which H_{irr} values for different temperatures can be determined. The linear extrapolation allows measurements of H_{irr} values above 9 T. The results are plotted in Fig. 2 for MgB₂ films of different carbon contents. For $H \perp ab$, H_{irr} is enhanced monotonically by carbon alloying to about 20 T at 4.2 K for the 15% carbon film.

The high H_{irr} in carbon-alloyed MgB₂ HPCVD films is likely due to the specific microstructures of the HPCVD

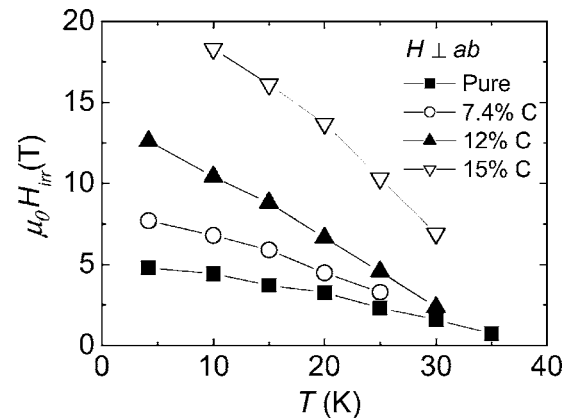


FIG. 2. Temperature dependence of H_{irr} with the $H \perp ab$ plane for pure and carbon-alloyed MgB₂ films.

films. We have shown previously by x-ray diffraction and transmission electron microscopy that the carbon-alloyed films are textured (c axis normal to the film surface) with columnar $\text{Mg}(\text{B}_{1-x}\text{C}_x)_2$ nanograins and highly resistive boron carbide (most likely B_4C , B_8C , or B_{13}C_2) grain boundaries.^{23,24} Unlike carbon-doped single crystals, where the a axis lattice constant decreases but that of the c axis remains almost constant or slightly increases,^{31,32} both the c and a axes in the carbon-alloyed HPCVD films expand with increasing carbon content.²³ Because only a small portion of carbon is doped into the $\text{Mg}(\text{B}_{1-x}\text{C}_x)_2$ grains, the carbon content dependence of the superconducting and transport properties of the HPCVD films is also very different from those in carbon-doped single crystals, where T_c is suppressed to 2.5 K at a residual resistivity of $50 \mu\Omega \text{ cm}$ when 12.5 at. % of carbon is doped into MgB_2 .³¹ The resistivity increase is much more dramatic and the T_c decrease is much slower with carbon content in the HPCVD films. These differences are likely related to the low carbon content in the MgB_2 phase and the presence of secondary phases in the grain boundaries. Both of these factors presumably contribute to the strong pinning and high H_{irr} in the HPCVD films.

Comparing the H_{irr} results with H_{c2} values of the films (where both are measured), we found that for $H \perp ab$, the ratio $H_{\text{irr}}(T)/H_{c2}(T)$ remains between 0.70 and 0.85 for all the pure and carbon-alloyed MgB_2 films, similar to the Nb-based superconductors ($H_{\text{irr}}/H_{c2} \sim 0.85$), and much larger than the high-temperature superconductors (H_{irr}/H_{c2} extremely small).⁹ In layered high-temperature superconductors, vortices are like weakly coupled “pancakes” that are easily depinned by thermal fluctuations.³³ In comparison, the anisotropy of MgB_2 is smaller³⁴ and the vortex lines are more continuous, therefore the thermal depinning is much weaker.

To understand the result displayed in Fig. 2, we examined the scaling behavior between the reduced pinning force $f = F_p/F_{p \text{ max}}$ and reduced field $h = H/H_{\text{irr}}$. When a dominant pinning mechanism exists, data from different measurement temperatures overlap and a scaling law of the form $f \propto h^n(1-h)^m$ is observed, which provides hints to the nature of the pinning.¹⁰ We found that for $H \perp ab$, scaling is observed for all the samples. It should be noted that for $H \parallel ab$, the $f(h)$ results of different temperatures do not overlap, suggesting that there is no dominant pinning mechanism when the applied field is in the ab plane. Lacking high-field data, we were therefore unable to obtain estimates of H_{irr} for $H \parallel ab$ from extrapolations of the flux pinning curves.

In Fig. 3, f versus h for $H \perp ab$ is plotted for the four films. For the pure MgB_2 film, the best fit, $f \propto h^{0.42}(1-h)^{1.87}$, is close to $h^{1/2}(1-h)^2$ for the grain boundary pinning.¹¹ Also, $F_{p \text{ max}} \propto H_{\text{irr}}^{2.28}$ is close to $F_{p \text{ max}} \propto H_{\text{irr}}^{2.5}$ for the grain boundary pinning.¹¹ A similar observation has also been reported in undoped polycrystalline bulk MgB_2 samples¹² and films.¹³ For the 7.4% carbon film, $f \propto h^{0.80}(1-h)^{2.23}$ and $F_{p \text{ max}} \propto H_{\text{irr}}^{1.58}$, similar to what has been observed in granular sputtered MgB_2 films.¹⁴ Values of $n=1$, $m=2$, and $F_{p \text{ max}} \propto H_{\text{irr}}^2$ have been associated with non-superconducting point pinning centers.¹⁰ For the 12% and 15% carbon films, the scaling behavior returns to that of the

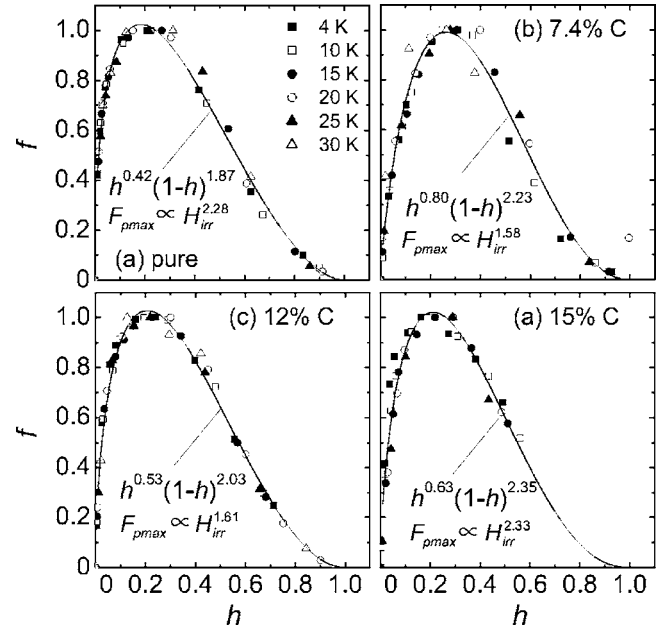


FIG. 3. Reduced pinning force, $f = F_p/F_{p \text{ max}}$, vs reduced field, $h = H/H_{\text{irr}}$, for the pure and carbon-alloyed MgB_2 films. The magnetic-field direction is the $H \perp ab$ plane. The solid lines are fittings to $f \propto h^n(1-h)^m$.

grain boundary pinning with $n \sim 0.5$ and $m \sim 2$. Similar changes from grain boundary pinning to normal point pinning and back to grain boundary pinning have been observed in neutron irradiated polycrystalline bulk MgB_2 .³⁵

It has been established that the HPCVD MgB_2 films grow initially as separated islands that coalesce at larger film thicknesses.³⁶ Given that the pure HPCVD MgB_2 films are very clean,²² grain boundaries formed during the film growth, aligned normal to the ab plane, will be the main pinning centers when $H \perp ab$. Carbon alloying dopes the MgB_2 grains, generates point defects, modifies the grain boundaries, and changes the grain size.²³ At the low carbon content, 7.4%, the results suggest that normal point pinning centers are being introduced that provide stronger pinning than the grain boundaries. At higher carbon content, the precipitate size becomes of order tens of nanometers,²³ making them ineffective as pinning centers. It is therefore likely that for these higher carbon concentrations, the boron-carbide containing grain boundaries²⁴ are once again the dominant pinning centers. That is, it appears that at low carbon concentrations we introduce point pinning centers that coarsen with increasing carbon content, causing the dominant pinning mechanism to switch from point pinning to grain boundary pinning as the carbon level is increased. When the applied field is in the ab plane, the vortices are not aligned with the grain boundaries and no dominant pinning mechanism is observed.

The increase in the flux pinning by carbon alloying is also demonstrated in the enhanced activation energy of vortices by thermal fluctuation. At low currents where the I - V curves are linear, a linear dependence $\ln \rho \propto 1/T$ indicates a thermally activated flux motion^{37,38} with the slope being the thermal activation energy U . In the inset to Fig. 4, an Arrhenius

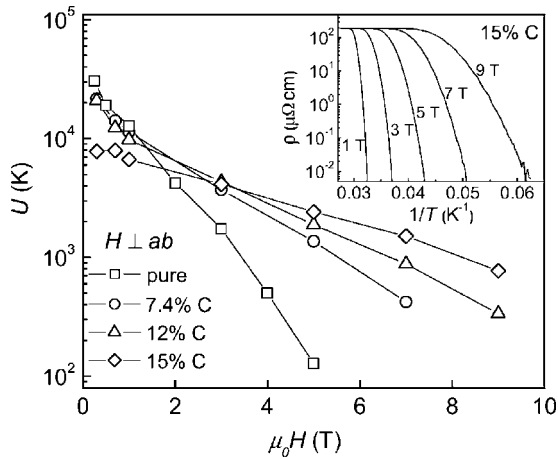


FIG. 4. Vortex activation energy as a function of applied magnetic field for pure and carbon-alloyed MgB_2 films. Inset: Arrhenius plot for the film with 15% carbon content. The magnetic field direction is $H \perp ab$.

plot is shown for the 15% carbon film. The magnetic-field direction is $H \perp ab$. In Fig. 4, U versus H is plotted for the pure and carbon-alloyed MgB_2 films. At zero and low fields, U decreases upon carbon alloying due to reduction in the superconducting condensation energy by carbon doping. At high fields, the carbon-alloyed films show much slower suppression of U by magnetic field and consequently much higher U , indicating much stronger flux pinning than in the pure MgB_2 film.

The stronger pinning in the carbon-alloyed MgB_2 films leads to a significant improvement in the high-field critical current density. Figure 5 shows $J_c(H)$ for four films at (a) 4.2 K and (b) 25 K with $H \perp ab$. The perpendicular field suppresses H_{c2} (Refs. 6 and 34) and $J_c(H)$ (Ref. 5) more strongly than a parallel field. For the pure MgB_2 film, the self-field J_c is very high, over 10^7 A/cm², but it drops quickly in magnetic field. When alloyed with carbon, the self-field and low-field J_c decreases with carbon content due to the reduction in the low-field activation energy as well as the decrease in the current-carrying cross-section area.²⁴ However, the suppression of J_c by magnetic field is much weaker in carbon-alloyed films. Consequently, the high-field J_c is significantly enhanced. For example, in the 12% carbon film, $J_c(T=4.2 \text{ K}, \mu_0 H=9 \text{ T})=4 \times 10^4$ A/cm² and $J_c(T=25 \text{ K}, \mu_0 H=3 \text{ T})=3 \times 10^4$ A/cm², whereas J_c in the pure MgB_2 film has already diminished at these temperatures and fields. A similar trend has also been observed in the parallel field. It should be noted that the magnitude of J_c is also affected by the area fraction of MgB_2 within the sample. As more carbon is added to the film, the increase in the number of secondary phase precipitates can block the current pathway. Thus the optimum carbon concentration for high $J_c(H)$ is a compromise between enhanced H_{c2} , H_{irr} , and flux pinning, and the effective superconducting cross section.

Carbon alloying also leads to a decrease in the anisotropy of $J_c(H)$. Figure 6 plots $J_c(H)$ for both $H \parallel ab$ and $H \perp ab$ at 15 K for the pure samples and all three samples with carbon additions. The anisotropy decreases monotonically with increasing carbon content. For the 15% carbon film, $J_c(H)$ is

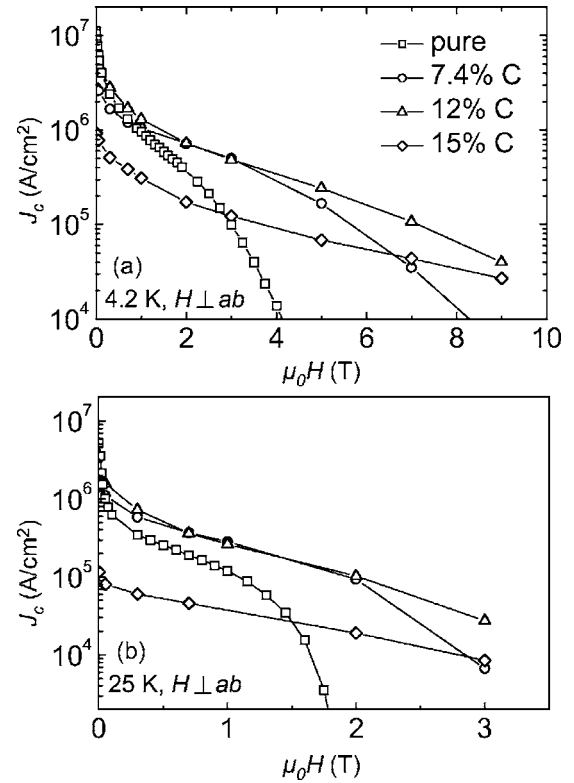


FIG. 5. Critical current density as a function of applied magnetic field for pure and carbon-alloyed MgB_2 films. (a) $T=4.2$ K and (b) $T=25$ K. The magnetic-field direction is $H \perp ab$.

isotropic. As can be seen, this is primarily the result of substantial enhancement of flux pinning for the $H \perp ab$ direction, while the change in the magnetic-field dependence for $H \parallel ab$ is much smaller.

Although we were unable to accurately ascertain the behavior of H_{irr} for $H \parallel ab$ from the $J_c^{1/2} H^{1/4}$ versus H plots, we have measured transport properties of carbon-alloyed MgB_2

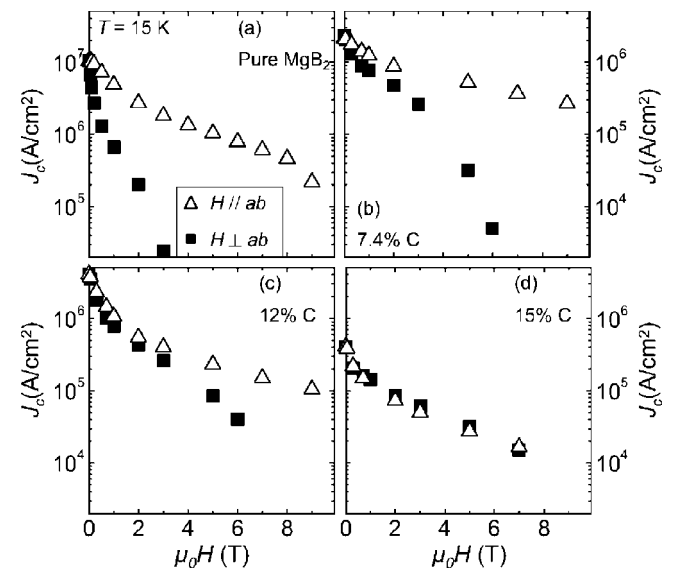


FIG. 6. Critical current densities as a function of applied magnetic field measured. Data shown are for $H \parallel ab$ and $H \perp ab$ at 15 K.

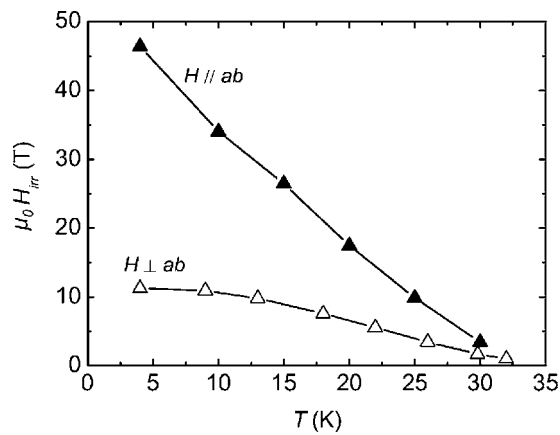


FIG. 7. Irreversibility fields, determined from transport measurements, for a sample containing a total carbon concentration of approximately 25%.

films with higher total carbon concentrations in pulsed high magnetic field up to 60 T. From these measurements we determined H_{irr} values using a resistivity criteria of 10% of the normal-state resistivity. In samples containing a total carbon concentration near 25%, H_{irr} for $H \parallel ab$ reaches values near 45 T at 4.2 K (Fig. 7), which is considerably higher than any previously reported H_{irr} values in MgB_2 (25.4 T at 4.2 K in MgB_2 wires with SiC nanoparticle additions¹⁹), and much higher than those in Nb-Ti and Nb₃Sn.³⁹ It should be noted that this sample has an H_{irr} for $H \perp ab$ near 10 T at 4.2 K, which is less than the values obtained in the case of 12% and 15% carbon additions reported above. That H_{irr} for $H \perp ab$ decreases for even higher concentrations of carbon is not surprising as it has been shown that, due to an increase in the amount of secondary phases, the area fraction of MgB_2 drops below 50% for carbon levels above approximately 15%.²⁴ This, coupled with the coarsening of the precipitate size with

increased carbon concentration,²³ should lead to a decrease in both the strength of the flux pinning and the overall critical current density. These data suggest that H_{irr} for $H \perp ab$ may be maximum for samples with a total carbon concentration near 12–15%, and H_{irr} for $H \parallel ab$ may achieve values even higher than 45 T. This subject warrants further investigation due to the potential applicability of MgB_2 to generate high magnetic fields.

IV. CONCLUSIONS

We have found that carbon alloying significantly enhances flux pinning in HPCVD MgB_2 films. The dominant pinning mechanism changes from the grain boundary pinning in pure MgB_2 films to normal point pinning at low carbon content and back to grain boundary pinning at higher carbon content for $H \perp ab$. No dominant pinning mechanism exists when $H \parallel ab$, but transport measurement shows that H_{irr} for $H \parallel ab$ reaches values near 45 T at 4.2 K in films of about 25% carbon concentration. The changes in the microstructure cause the enhancement of flux pinning. Enhanced flux pinning in carbon-alloyed films results in substantially higher J_c at high fields than in the pure MgB_2 films. The results demonstrate that by optimizing the carbon content, carbon-alloyed HPCVD MgB_2 films can achieve remarkably high values of H_{c2} , H_{irr} , and $J_c(H)$, significantly raising the prospect of MgB_2 as a practical high-magnetic-field material.

ACKNOWLEDGMENTS

We thank David Larbalestier for helpful comments on the manuscript. This work is supported in part by NSF under Grants No. DMR-0405502 (Q.L.), and No. DMR-0306746 (X.X. and J.M.R.), and by ONR under Grants No. N00014-00-1-0294 (X.X.) and No. N0014-01-1-0006 (J.M.R.).

*Electronic address: qill@psu.edu

¹J. Nagamatsu, N. Nakagawa, T. Muranaka, Y. Zenitani, and J. Akimitsu, *Nature (London)* **410**, 63 (2001).
²Y. Iwasa, D. C. Larbalestier, M. Okada, R. Penco, M. D. Sumpston, and X. X. Xi, *IEEE Trans. Appl. Supercond.* **16**, 1457 (2006).
³H. J. Choi, D. Roundy, H. Sun, M. L. Cohen, and S. G. Louie, *Nature (London)* **418**, 758 (2002).
⁴A. Gurevich, *Phys. Rev. B* **67**, 184515 (2003).
⁵X. H. Zeng *et al.*, *Nat. Mater.* **1**, 35 (2002).
⁶V. Braccini *et al.*, *Phys. Rev. B* **71**, 012504 (2005).
⁷R. H. T. Wilke, S. L. Bud'ko, P. C. Canfield, D. K. Finnemore, and S. T. Hannahs, *Physica C* **424**, 1 (2005).
⁸S. X. Dou, V. Braccini, S. Soltanian, R. Klie, Y. Zhu, S. Li, X. L. Wang, and D. Larbalestier, *J. Appl. Phys.* **96**, 7549 (2004).
⁹D. C. Larbalestier, A. Gurevich, D. M. Feldmann, and A. A. Polyanskii, *Nature (London)* **414**, 368 (2001).
¹⁰D. Dew-Hughes, *Philos. Mag.* **30**, 293 (1974).
¹¹D. Dew-Hughes, *Philos. Mag. B* **55**, 459 (1987).
¹²D. C. Larbalestier *et al.*, *Nature (London)* **410**, 186 (2001).

¹³A. Gupta, H. Narayan, D. Astill, D. Kanjilal, C. Ferdeghini, M. Paranthaman, and A. V. Narlikar, *Supercond. Sci. Technol.* **16**, 951 (2003).
¹⁴S. L. Prischepa, M. L. Della Rocca, L. Maritato, M. Salvato, R. Di Capua, M. G. Maglione, and R. Vaglio, *Phys. Rev. B* **67**, 024512 (2003).
¹⁵R. H. T. Wilke, S. L. Bud'ko, P. C. Canfield, D. K. Finnemore, R. J. Suplinskas, and S. T. Hannahs, *Phys. Rev. Lett.* **92**, 217003 (2004).
¹⁶M. Angst, R. Puzniak, A. Wisniewski, J. Jun, S. M. Kazakov, J. Karpinski, J. Roos, and H. Keller, *Phys. Rev. Lett.* **88**, 167004 (2002).
¹⁷E. Ohmichi, E. Komatsu, T. Masui, S. Lee, S. Tajima, and T. Osada, *Phys. Rev. B* **70**, 174513 (2004).
¹⁸A. Serquis *et al.*, *Appl. Phys. Lett.* **82**, 2847 (2003).
¹⁹M. D. Sumpston, M. Bhatia, M. Rindfliesch, M. Tomsic, S. Soltanian, S. X. Dou, and E. W. Collings, *Appl. Phys. Lett.* **86**, 092507 (2005).
²⁰V. Ferrando, P. Orgiani, A. V. Pogrebnyakov, J. Chen, Q. Li, J. M. Redwing, and X. X. Xi, *Appl. Phys. Lett.* **87**, 252509 (2005).

- ²¹M. Eisterer, M. Zehetmayer, and H. W. Weber, *Phys. Rev. Lett.* **90**, 247002 (2003).
- ²²A. V. Pogrebnyakov, J. M. Redwing, J. E. Jones, X. X. Xi, S. Y. Xu, Q. Li, V. Vaithyanathan, and D. G. Schlom, *Appl. Phys. Lett.* **82**, 4319 (2003).
- ²³A. V. Pogrebnyakov *et al.*, *Appl. Phys. Lett.* **85**, 2017 (2004).
- ²⁴A. V. Pogrebnyakov *et al.*, *IEEE Trans. Appl. Supercond.* **15**, 3321 (2005).
- ²⁵C. B. Eom *et al.*, *Nature (London)* **411**, 558 (2001).
- ²⁶V. Braccini, L. D. Cooley, S. Patnaik, D. C. Larbalestier, P. Manfrinetti, A. Palenzona, and A. S. Siri, *Appl. Phys. Lett.* **81**, 4577 (2002).
- ²⁷J. E. A. Gümbel, G. Fuchs, K. Nenkov, K.-H. Müller, and L. Schultz, *Appl. Phys. Lett.* **80**, 2725 (2002).
- ²⁸A. Yamamoto, J. Shimoyama, S. Ueda, Y. Katsura, I. Iwayama, S. Horii, and K. Kishio, *Appl. Phys. Lett.* **86**, 212502 (2005).
- ²⁹M. D. Sumption, M. Bhatia, S. X. Dou, M. Rindfliesch, M. Tomasic, L. Arda, M. Ozdemir, Y. Hascicek, and E. W. Collings, *Supercond. Sci. Technol.* **17**, 1180 (2004).
- ³⁰E. J. Kramer, *J. Appl. Phys.* **44**, 1360 (1973).
- ³¹S. Lee, T. Masui, A. Yamamoto, H. Uchiyama, and S. Tajima, *Physica C* **397**, 7 (2003).
- ³²M. Avdeev, J. D. Jorgensen, R. A. Ribeiro, S. L. Bud'ko, and P. C. Canfield, *Physica C* **387**, 301 (2003).
- ³³G. Blatter, M. V. Feigelman, V. B. Geshkenbein, A. I. Larkin, and V. M. Vinokur, *Rev. Mod. Phys.* **66**, 1125 (1994).
- ³⁴M. Angst, R. Puzniak, A. Wisniewski, J. Jun, S. M. Kazakov, J. Karpinski, J. Roos, and H. Keller, *Phys. Rev. Lett.* **88**, 167004 (2002).
- ³⁵I. Pallecchi *et al.*, *Phys. Rev. B* **71**, 212507 (2005).
- ³⁶A. V. Pogrebnyakov *et al.*, *Phys. Rev. Lett.* **93**, 147006 (2004).
- ³⁷M. Tinkham, *Introduction to Superconductivity* (McGraw-Hill, New York, 1975).
- ³⁸S. Patnaik, A. Gurevich, S. D. Bu, S. D. Kaushik, J. Choi, C. B. Eom, and D. C. Larbalestier, *Phys. Rev. B* **70**, 064503 (2004).
- ³⁹M. Suenaga, A. K. Ghosh, Y. Xu, and D. O. Welch, *Phys. Rev. Lett.* **66**, 1777 (1991).